Centella Asiatica Ameliorates Radiation-induced Epithelial Barrier Dysfunction by Secreting Epidermal Growth Factor in Endothelial Cells.

Seo Young Kwak
Korea Institute of Radiological & Medical Sciences https://orcid.org/0000-0003-1252-3549
Sehwan Shim
Korea Institute of Radiological & Medical Sciences
Won Il Jang
Korea Institute of Radiological & Medical Sciences
Seung Bum Lee
Korea Institute of Radiological & Medical Sciences
Min-Jung Kim
Korea Institute of Radiological & Medical Sciences
Sunhoo Park
Korea Institute of Radiological & Medical Sciences
Sang Sik Cho
Korea Institute of Radiological & Medical Sciences
Hyewon Kim
Korea Institute of Radiological & Medical Sciences
Sun-Joo Lee
Korea Institute of Radiological & Medical Sciences
Hyosun Jang (hsjang@kirams.re.kr)
Korea Institute of Radiological and Medical Sciences (KIRAMS) https://orcid.org/0000-0002-5910-5099

Research

Keywords: Centella asiatica, radiation-induced enteropathy, epithelial barrier dysfunction, epidermal growth factor, endothelial secretome, crosstalk between endothelial, epithelial cells

Posted Date: September 29th, 2021

DOI: https://doi.org/10.21203/rs.3.rs-929863/v1

Abstract

Background

Radiation-induced intestinal damage is frequently observed following radiotherapy for abdominal and pelvic cancer or occurs due to radiation exposure in a nuclear accident. In an effort to overcome radiation-induced normal tissue damage, a variety of radio-mitigator candidates have been investigated. The loss of the epithelium and its barrier function leads to 'leaky gut', so recovery of damaged epithelium is an important strategy in therapeutic trials. *Centella asiatica* (CA), a traditional herbal medicine in Chinese culture, is widely used for wound healing by protecting against endothelial damage. In this study, we investigated the radio-mitigating effect of CA, focusing on crosstalk between endothelial and epithelial cells.

Results

CA treatment attenuated radiation-induced endothelial dysfunction in human umbilical vein endothelial cells and mitigated radiation-induced enteropathy in a mouse model. In particular, treatment of the conditioned media from CA-treated irradiated endothelial cells recovered loss of epithelial integrity by regulating zonula occludens 1 and desmoglein 2 in radiation exposure. We also determined that epidermal growth factor (EGF) is a critical factor secreted by CA-treated irradiated endothelial cells. Treatment with EGF, which can mimic the effect of CA-induced secretion in irradiated endothelial cells, effectively improved the radiation-induced epithelial barrier dysfunction. In addition, blockade of EGF in CA-induced endothelial secretome impeded epithelial barrier recovery. Finally, we identified the therapeutic effects of CA-induced endothelial secretome in a radiation-induced enteropathy mouse model with epithelial barrier restoration.

Conclusions

We have shown therapeutic effects of CA on radiation-induced enteropathy, with the recovery of endothelial and epithelial dysfunction, focusing on the crosstalk between endothelial cells and epithelial cells. Thus, our finding suggest that CA is an effective radio-mitigator against radiation-induced enteropathy.

Background

Radiation-induced intestinal injury is observed following clinical application of radiation for pelvic cancer or radiation exposure in a nuclear accident. Severe intestinal damage, with insufficient epithelial cell production and instability [1, 2], leads to side effects like vomiting, weight loss, diarrhea, infections, and septic shock-induced death [3]. The endothelium has been described as an important component involved in gastrointestinal (GI) disease [4], and it has been proposed that the pathogenesis of radiation-induced enteropathy is associated with endothelial dysfunction and death [5–7]. Meanwhile, prevention of endothelial cell damage by growth factors, such as vascular endothelial cell growth factor or basic

fibroblast growth factor, results in reduction of intestinal crypt cell damage, inflammation, organ failure, and death in radiation-induced GI toxicity [8].

The epithelium in the intestine is anatomically positioned in close proximity to a number of sub epithelial cell types, including endothelia. Crosstalk between epithelial cells and these sub epithelial cell populations contributes to epithelial function through paracrine signaling [9–12]. The secretome is defined as a subset of a proteome that contains all proteins that are actively exported from the cell. Typically, secreted protein plays a direct autocrine and/or paracrine role in a broad range of biological processes, including homeostasis, developmental regulation, immune defense, development of the extracellular matrix, and signal transduction [13–15].

The epithelial barrier is the first line of defense in the GI tract that prevents the diffusion of pathogens into intestinal mucosa. Radiation-induced tissue damage and disrupted healing result in alteration of the tissue architecture and functions. Protein-protein networks connect epithelial cells, thereby forming intracellular junctions that include the adherens junction (AJ), tight junction (TJ), and desmosome [16]. Paracellular permeability across the epithelial cells is regulated by TJ, whereas AJ participates in cell-cell adhesive interactions [17]. Epithelial cells also form desmosomes that are involved in strength adhesive interactions [18, 19]. Factors that prevent epithelial barrier dysfunction are important in developing therapeutic drugs for the radiation-induced GI damage [20–22].

Centella asiatica (CA), known as Asiatic pennywort, is widely used as a traditional herbal medicine in China and Indian. This tropical medicinal plant is enriched with bioflavonoids, triterpenes, and selenium and has been reported to promote healing for ulceration, diarrhea, mental clarity, depression, and skin psoriasis [23–26]. In recent years, much attention has been paid to the potential of CA in the treatment of various types of disease and some putative mechanisms have been proposed, including antioxidant and lipid metabolism in the skin and neurons [27, 28]. Importantly, it has also been reported that CA can protect endothelial cells, increase cell proliferation, inhibit apoptosis of endothelial cells, and block beta-amyloid peptide aggregation [29]. Madecassoside, one of the triterpines isolated from CA, is known to preserve endothelial cells from oxidative injury by protection of mitochondria membrane potential and apoptosis [30]. Tumor necrosis factor-alpha from asiatic acid, which is the other triterpene in CA, attenuates endothelial barrier dysfunction, thereby resulting in prevention of atherosclerosis [31]. However, the effect of CA on radiation-induced endothelial cell damage has not yet been investigated.

The results of the present study show that CA ameliorated radiation-induced enteropathy with recovery of endothelial cell damage and epithelial barrier dysfunction. We hypothesized that the soluble factor secreted by CA-treated irradiated endothelial cells could repair the radiation-induced enteropathy by regulating the epithelial barrier. We found that the conditioned media (CM) of CA-treated irradiated endothelial cells reversed the radiation-induced epithelial barrier dysfunction in vitro as well as in the radiation-induced enteropathy in a mouse model. We also discovered that CA treatment of irradiated endothelial cells induced the secretion of epidermal growth factor (EGF), which is necessary for the repair of radiation-induced epithelial barrier dysfunction, including integrity and expression of junction proteins.

Of particular note, blocking EGF in CM using a neutralizing antibody failed to rescue the epithelial barrier dysfunction. Collectively, the results demonstrate that CA ameliorated radiation-induced enteropathy by regulating endothelial cell secretome.

Results

CA attenuates radiation-induced endothelial dysfunction.

To investigate the radio-mitigator effects of CA on irradiated endothelial cells, we performed several assays using human umbilical vein endothelial cells (HUVECs) in the presence or absence of CA. We used the CCK-8 assay in irradiated HUVECs to assess cell proliferation. Irradiation of HUVECs showed a significant downregulation of cell proliferation compared to the control, but CA treatment rescued the radiation-induced loss of cell proliferation (Fig. 1A, B). Because radiation induces cellular senescence [32], we tested the cellular senescence activity using a β-galactosidase (β-gal) assay. The β-gal activity was observed in irradiated HUVECs, but CA treatment of irradiated HUVECs displayed lower β-gal activity than irradiated HUVECs (Fig. 1C). A tube formation assay was performed to assess angiogenic capacity. Tube-forming activity of HUVECs was inhibited by radiation, but CA treatment restored the angiogenic activity of irradiated HUVECs (Fig. 1D). These results suggest that CA mitigated radiation-induced endothelial dysfunction, including proliferation, senescence, and angiogenic properties.

CA mitigates radiation-induced enteropathy in mouse model.

We evaluated the therapeutic effects of CA in mice using a radiation-induced enteropathy mouse model in which the abdomen of the mouse was irradiated. Mice were then either treated with CA or left untreated. Six days after irradiation, the effect of CA on radiation-induced enteropathy was determined using physiological and histological examinations. CA administration to the irradiated mouse attenuated loss of body weight compared to the irradiated group (Fig. 2A). Histological analyses of irradiated intestine showed shorter villi length and crypt disruption, whereas CA treatment restored villi length and crypt numbers in irradiated mice (Fig. 2B, C). Histological scoring, accomplished by evaluating epithelial structural damage, vascular dilation, and inflammatory cell infiltration in the mucosa and submucosa, was lower in CA-treated irradiated mice than the irradiated group (Fig. 2D). Immunohistochemical activity for Ki-67, a proliferation marker, was also increased in the CA-treated irradiated mouse group compared to the irradiated group (Fig. 2E). As indicated by immunohistochemistry for the endothelial cell marker CD31, angiogenic activity was also higher in CA-treated irradiated mice than in the irradiated group (Fig. 2F). Taken together, these results suggest that CA alleviates radiation-induced enteropathy with restoration of endothelial dysfunction.

CA attenuates radiation-induced intestinal barrier dysfunction in mouse model.

The epithelial barrier requires a monolayer of epithelial cells to separate organs from the extracellular environment. An intact epithelium plays a pivotal role in defense against exogenous pathogens. Conversely, impaired intestinal epithelial barrier function is a hallmark of GI diseases, such as

inflammatory bowel disease and celiac disease [33–36]. Based on the aforementioned knowledge, we investigated whether CA affects radiation-induced intestinal barrier dysfunction in a mouse model system. We evaluated bacterial translocation in mesenteric lymph nodes as a measure of the integrity of the intestinal barrier. The bacterial translocation in the mesenteric lymph nodes was increased in the irradiated mouse group compared to the control group, but it was decreased in the CA-treated mouse group compared to the irradiated group (Fig. 3A). Next, we assessed expressions of the several molecules regulating the barrier function. Immunohistochemistry analysis showed that cells positive for epithelial barrier-related molecules, such as villin, zonula occludens 1 (Zo1), Desmoglein 2 (Dsg2), and Claudin 3 (Cldn3), were decreased in the irradiated group compared to the control group. However, these expressions were restored in the CA-treated group (Fig. 3B). We also assessed mRNA levels of these molecules in intestinal tissue. The mRNA levels of epithelial barrier-related molecules in the irradiated mouse group showed a significantly lower expression compared to the control group, but CA treatment restored mRNA expression (Fig. 3C). Taken together, these results suggest that CA attenuated radiation-induced enteropathy thereby avoiding intestinal barrier dysfunction in a mouse model.

Secretome of CA-treated endothelial cells repairs epithelial barrier dysfunction.

The epithelium, which is considered to be responsible for protection against exogenous pathogen, is constantly exposed to soluble factors produced by surrounding cells in the microenvironment [37–39]. Considering CA alleviates radiation-induced enteropathy with improvement of endothelial cell function in vitro, it was decided to evaluate the functional effect of a CA-treated endothelial cell secretome on epithelial cell damage repair. We used well-established in vitro models reflecting epithelial barriers [40, 41] to evaluate the functional activity of endothelial cell secretome on a damaged epithelial barrier. The CM of HUVECs was collected after irradiation (IR) or irradiation followed by CA treatment (IR + CA) in serum-free medium. The CM of each sample was tested on a Caco-2 monolayer. As shown in Fig. 4A, the transepithelial electrical resistance (TEER) value of the CM from IR HUVECs-treated irradiated Caco-2 monolayers was decreased compared with that of IR HUVECs-treated non-irradiated Caco-2 monolayer. Otherwise, the CM of IR + CA HUVECs treatment increased the TEER value in irradiated Caco-2 monolayers (Fig. 4A). In addition, Fluorescein isothiocyanate (FITC) flux of the CM of IR HUVECs-treated irradiated Caco-2 monolayers was increased compared to the CM of IR HUVECs-treated non-irradiated Caco-2 monolayers. The CM of IR + CA HUVECs treatment on irradiated Caco-2 monolayers decreased FITC flux in FITC-dextran assay (Fig. 4B). The cell-cell contact strength of irradiated Caco-2 monolayers was also improved by the CM of IR + CA HUVECs treatment (Fig. 4C). We used immunofluorescence to evaluate the expression of barrier integrity-related molecules. In the mouse model, we identified that CA markedly upregulated Cldn3 expression in irradiated intestine. Unfortunately, loss of CLDN3 was not rescued by the CM of IR + CA HUVECs treatment in irradiated Caco-2 monolayers (data not shown). Although ZO1 and DSG2 were lost in the junctions of the CM of IR HUVECs-treated irradiated Caco-2 monolayers, the loss of junctional molecules was recovered by CM of IR + CA HUVECs treatment of irradiated Caco-2 monolayers (Fig. 4D). Consistent with these results, protein and mRNA levels of ZO1 and DSG2 were decreased in the CM of IR HUVECs-treated irradiated Caco-2 monolayers, whereas these expressions were restored by treatment of the CM of IR + CA HUVECs (Fig. 4E, F). Collectively, CA

modulated the endothelial secretome to restore radiation-induced barrier dysfunction particularly that associated with ZO1 and DSG2.

EGF is identified as a key regulator of restoration of radiation-induced epithelial barrier dysfunction.

A number of studies have revealed that endothelial cells secrete a variety of biologically active growth factors, cytokine, extracellular matrix protein, and tissue remodeling enzymes [42]. The factors from endothelial cells may help restore the GI epithelium. To elucidate which secretory molecules influence the repair of radiation-induced epithelial dysfunction, we performed cytokine array experiments to analyze secretome profiling. Each CM of HUVECs [i.e., control (Con), irradiated HUVECs (IR), CA-treated HUVECs (CA), and CA-treated irradiated HUVECs (IR + CA)] was applied to the cytokine array. Cytokine analysis revealed changes in several factors, including EGF, interleukin (IL)-6, and IL-8 (Fig. 5A). Although IL-6 and IL-8 levels significantly decreased in the IR + CA group compared to the IR group, there was no response to irradiation. The EGF level decreased in the IR group compared with Con group and was significantly upregulated in the IR + CA group compared with the IR group. A well-known growth factor, EGF plays critical roles in cell proliferation and protects the GI mucosa from a variety of insults [43, 44]. EGF has also shown to regulate a number of GI functions, defining its physiologic role in the GI tract [45–48]. The quantity of EGF, determined using an enzyme-linked immunosorbent assay (ELISA), was significantly increased 2-fold in the IR + CA group compared to the IR group (Fig. 5B). EGF-positive HUVECs increased in immunofluorescence in the IR + CA group compared to the IR group (Fig. 5D). The mRNA level of *EGF* was also decreased in the IR group, but its expression was recovered in the IR + CA group (Fig. 5C). These results suggest that CA treatment of irradiated endothelial cells induced EGF production and secretion.

EGF relieved radiation-induced epithelium barrier dysfunction.

A functional assay was performed by exposing recombinant EGF (rEGF) to determine whether CA-induced endothelial EGF secretion could ameliorate radiation-induced epithelium barrier dysfunction. The results indicated that the decreased TEER value in irradiated Caco-2 monolayers was increased by exposure to rEGF (Fig. 6A). An FITC-dextran assay indicated that FITC flux was elevated in media of irradiated Caco-2 monolayers, but it was diminished by rEGF treatment (Fig. 6B). Cell-cell contact strength was decreased in irradiated Caco-2 cell monolayers, but enhanced when rEGF was exposed to irradiated Caco-2 cell monolayers (Fig. 6C). Confocal staining revealed that immunohistochemical activities against ZO1 and DSG2 were diminished in the cellular junction of irradiated Caco-2 monolayers but were reinforced by rEGF treatment (Fig. 6D). The protein and RNA levels of ZO1 and DSG2 had the same pattern as the confocal staining result (Fig. 6E, F). EGF treatment of endothelial cells was also tested due to the possibility of an autocrine mode. The results indicate that rEGF treatment to HUVECs did not induce any mitigating effects like proliferation, anti-senescence, and angiogenic ability (supplement Fig. 1A-C). These results indicate that EGF, secreted by CA-treated irradiated HUVECs, reverts radiation-induced epithelial barrier dysfunction.

Endothelial-secreted EGF by CA treatment rescues radiation-induced barrier impairment with ZO1 and DSG2 regulation.

To examine whether EGF blockade in the CM of CA-treated irradiated HUVECs impeded the repair of epithelial barrier dysfunction, we abolished EGF in the CM of CA-treated HUVECs using a neutralizing antibody (anti-EGF). As shown in Fig. 7A, inhibition of EGF in CM of IR + CA HUVECs significantly reduced the TEER value compared with CM of IR + CA HUVECs treatment. Blocking of EGF also failed to decrease the FITC flux of CM of IR + CA HUVECs-treated irradiated Caco-2 monolayers (Fig. 7B). A dispase-based dissociation assay showed that reinforcement of cell-cell contact strength in the CM group of IR + CA HUVECs was abolished by neutralizing EGF (Fig. 7C). Similarly, expression of epithelial barrier-related molecules in the CM group of anti-EGF treatment did not increase as much as the CM group of IR + CA (Fig. 7D, E). Upregulated mRNA levels of *ZO1* and *DSG2* in the CM group of IR + CA HUVECs were also abolished by anti-EGF treatment (Fig. 7F). These results indicate that CA-induced endothelial EGF rescues radiation-induced epithelial barrier impairment with ZO1 and DSG2 regulation.

CM of CA-treated endothelial cells mitigates radiation-induced enteropathy with epithelial barrier restoration in mouse model.

To evaluate the therapeutic effect of CA-induced endothelial EGF on radiation-induced enteropathy, we administered the CM of IR + CA HUVECs to an irradiated mouse model. The mouse groups were as follows: control (Con), irradiated (IR), irradiated and injected with the CM of irradiated HUVECs (IR + CM), irradiated and injected with the CM of CA-treated irradiated HUVECs (IR + CA-CM), and irradiated and injected with rEGF (IR + rEGF). Histological examination revealed that villi shortening and crypt disruption by radiation were rescued in the IR + CA-CM groups. Elevated histological scoring in the IR group was significantly reduced in the IR + CA-CM and IR + rEGF groups (Fig. 8A, C). Otherwise, there were no significant differences in the IR and IR + CM groups (Fig. 8A, C). Immunoreactivity for Ki-67 as a proliferating marker was also increased in the IR + CA-CM and IR + rEGF groups than the IR + CM group (Fig. 8B). Physiological examination showed that the body weight of the IR + CA-CM group was higher than that of the IR group at days 5 and 6 following treatment (Fig. 8D). Of particular note, the immunohistochemical activity to Villin, Zo1, Dsg2, and Cldn3 was increased in the IR + CA-CM and IR + rEGF groups compared to the IR group (Fig. 8E). The mRNA levels, including *Villin*, *Zo1*, *Dsg2*, and *Cldn3*, in intestinal tissue were also increased in the IR + CA-CM and IR + rEGF groups compared to the IR group (Fig. 8F). These results suggest that CA-induced endothelial EGF efficiently alleviates radiation-induced enteropathy and rescues the barrier dysfunction.

Discussion

Radiation is currently used as a component of therapy for a wide range of malignant conditions. Although the threat of nuclear terrorism is rare, it can happen, so it is necessary to prepare a countermeasure for radiation-induced damage. Radiation-induced intestinal injury, due to sensitive organ to radiation, leads to severe side effects, including vomiting, diarrhea, bacterial infection, and septic shock-induced death. Radiation-induced enteropathy has increasing morbidity and mortality, and such conditions require development of therapeutic reagents, such as radiation-protector or radio-mitigator.

Despite advances in radio-protectors (e.g., amifostine for acute radiation syndrome), there are no promising agents for an effective radio-mitigator.

The potential medicinal plant CA is widely used in traditional medicine in the Orient and has been applied to skin lesions, ulcerations, and diarrhea [25, 26]. In addition, its active constituents, primarily the main chemical components of pentacyclic triterpene derivatives (e.g., asiaticoside, asiatic acid, madecassoside, and madecassic acid have been reported to recover the damaged tissue [49]. Madecassoside has been reported to protect endothelial cells against oxidative stress [30], and asiaticoside has been reported to heal the incision through the formation of epithelial layer [50]. These reports indicate that CA is a promising reagent for the rescue of damaged tissues.

The effect of CA on survival rate against irradiation during clinical radiotherapy has been reported [51]. Treatment of Swiss albino with CA as a radioprotector at a sublethal dose of Co-60 gamma irradiation has been shown to prolong the survival rate [52]. Administration of CA has a dramatic radioprotection effect on radiation-induced body weight loss and conditioned taste aversion [53]. However, no studies have been reported on the effect of CA on radiation-induced enteropathy. In present study, we investigated the radio-mitigating effect of CA, focusing on crosstalk between endothelial and epithelial cells in vitro and in a mouse model. We found that CA ameliorates radiation-induced enteropathy through modulation of radiation-induced endothelial cell secretome. We also identified EGF as an endothelial cell driven-key regulator to repair radiation-induced epithelium disruption. Our findings also demonstrate that endothelial-derived EGF by CA treatment improved the epithelial barrier damage on radiation-induced enteropathy.

Interactions between intestinal epithelial cells and the subepithelial cellular components play important roles in controlling intestinal barrier function under pathological conditions [10, 54]. Studies have shown that crosstalk between endothelia and epithelial barrier is critical for regulation of tissue homeostasis and protection against pathogens or tissue damaging agent in human airways [55]. The endothelial-epithelial biochemical crosstalk pathway was studied using a human intestinal crypt cell line grown in noncontact co-culture with HUVEC. Endothelial cells secreted the 6-keto-prostaglandin F 1 alpha, a stable hydrolysis product of prostacyclin, resulting in epithelial cell activation through paracrine action [10]. In this study, we investigated the interactions between intestinal epithelial cells and endothelial cells in radiation exposure conditions. By applying the CM of CA-treated endothelial cells to irradiated epithelial cells, we demonstrated that the secretome of CA-treated endothelial cells could rescue the radiation-induced epithelial dysfunction.

EGF, a well-known monomeric peptide present in the GI lumen, plays important roles in mitogenesis in tissue [56–58]. EGF and its related peptides have been implicated in the promotion of cell proliferation in wound healing, such as in re-epithelialization [59, 60]. Furthermore, secreted EGF from bone marrow endothelial cells accelerates hematopoietic stem cell recovery [61]. It is well known that rEGF treatment promotes survival after radiation exposure [62] and protects radiation-induced enteropathy [63]. Otherwise, there is little information about the effects of EGF on radiation-induced epithelial barrier

damage. In our recent study, CA-induced EGF secretion rescued the impaired epithelial barrier in irradiated Caco-2 monolayers and in enteropathy mouse model. The use of EGF neutralizing antibody reversed the relieving effect and failed to rescue epithelial barrier dysfunction. Taken together, these findings indicated that CA-induced EGF was a modulator that contributed to recover the radiation-induced epithelial dysfunction. This is the first evidence for a functional cellular response of CA on damaged tissue.

Breakage of the epithelium barrier integrity is one of the important characteristics of radiation-induced enteropathy. Gut epithelial barrier is the first defense to protect the extra insults. It has been reported that the epithelial barrier damaged by radiation or inflammatory stimuli leads to downregulation of TEER and integrity, and fragmentation of cell-cell interactions [64, 65]. Complexes of intercellular junctions, including TJs (e.g., ZO1, CLDN3), AJs, and desmosomes (e.g., DSG2), are the principal components of the intestinal barrier. In particular, ZO1 alteration contributes to disturbance of epithelial barrier. Loss of ZO1 with barrier dysfunction has been shown in dextran sulfate sodium (DSS)-induced colitis and sepsis in a *pseudomonas aeruginosa* infection mouse model [66, 67]. Epithelial ZO1-deficient mice display severe mucosal damage with increased permeability following DSS application [68]. Also, DSG2 is required for the integrity of the intestinal epithelial barrier in vitro and in vivo [21, 22]. Intestinal epithelial DSG2 knockout mice exhibit severe colitis from DSS treatment with increasing intestinal permeability [22]. In this study, CA-induced EGF increased expression of ZO1 and DSG2 in irradiated Caco-2 monolayers and intestinal epithelium of radiation-induced enteropathy. Taken together, upregulation of ZO1 and DSG2 by CA-induced EGF contributes to the recovery of epithelial barrier damage in irradiation.

Conclusions

We found that CA attenuated radiation-induced endothelial dysfunction in vitro, including proliferation, senescence, and tube formation activity. We have also shown therapeutic effects of CA on radiation-induced enteropathy, with the recovery of endothelial and epithelial dysfunction, focusing on the crosstalk between endothelial cells and epithelial cells. In particular, we identified EGF, a key factor secreted by endothelial cells to repair radiation-induced epithelial barrier dysfunction. Furthermore, by using a neutralizing anti-EGF antibody, we have shown the failure of the restoration of the radiation-induced epithelial barrier dysfunction and the related molecules expression in Caco-2 monolayers. The CM of CA-treated HUVECs or rEGF was administrated to a mouse model, and the results show recovery of radiation-induced epithelial dysfunction, including increased expression of epithelial barrier-related molecules. Thus, our study results suggest the use of CA as an effective radio-mitigator against radiation-induced enteropathy.

Materials And Methods

Cell culture and reagents

HUVECs (Lonza, Basel, Switzerland) were cultured in EGM-2 medium supplemented with endothelial growth kit components (Lonza). Passage number of HUVECs used in experiments was between 4 and 7.

Human Caco-2 cells were maintained in Dulbecco's Modified Eagle Medium (DMEM, Gibco, Grand Island, NY, USA) supplemented with 10% fetal bovine serum (FBS, Gibco) and 1% antibiotics. All cells were grown in a humidified incubator at 37ºC with 5% humidity. Based on previous studies [41, 69], Caco-2 cells were grown into a confluent monolayer for in vitro experiments as a barrier function model. To obtain CM from HUVECs, irradiated HUVECs were either treated or not with CA (USP, MD, USA) for 24 h. After incubation, the media was exchanged with fresh serum-free EBM-2 media. Caco2 used in this study was between passage 18 and 33.

Animals

Specific pathogen-free male C57BL/6 mice were obtained from Harlan Laboratories (Indianapolis, IN, USA) and maintained in specific pathogen-free conditions at the KIRAMS animal facility. All mice were housed in a temperature-controlled room with a 12-h light/dark cycle. Food and water were provided *ad libitum*. The mice were acclimated for 1 week before commencement of the experiments and were grouped as follows: control (Con), irradiation (IR), irradiation with CA treatment (IR + CA), irradiation with CM from irradiated HUVECs treatment (IR + CM), irradiation with CM from CA-applied irradiated HUVECs treatment (IR + CA-CM), and irradiation with rEGF treatment (IR + rEGF). All animal experiments were approved and performed in accordance with the guidelines of the Institutional Animal Care and Use Committee of the Korea Institute of Radiological & Medical Sciences (KIRAMS; kirams 2020-0010).

Irradiation and treatment

Cells were irradiated to 10 or 15 Gy using a ^{137}Cs γ-ray source (Atomic Energy of Canada, Ltd, Canada) with a dose rate of 3.25 Gy/min. Animals were anesthetized with 85 mg/kg alfaxalone (Alfaxan®, Careside, Gyeonggi-do, Korea) and 10 mg/kg xylazine (Rompun® Bayer Korea, Seoul, Korea). Mice were irradiated in the abdomen with a single dose at 13.5 Gy using an X-RAD 320 X-ray irradiator (Softex, Gyeonggi-do, Korea). After exposure to radiation, CA (200 μg/kg/day), the CM of irradiated HUVECs, the CM of CA-treated irradiated HUVECs (200 μl/mouse/day), and rEGF (1 μg/mouse/day) were administrated for 6 days.

CCK-8 assay

HUVECs were seeded in a 96-well plate. On the next day, cells were irradiated at 10 Gy and treated with varying concentrations of CA. After a 48-h incubation, the CCK-8 reagent was added and measured using a microplate reader at a wavelength of 450 nm. The experiments were carried out at least in triplicate.

β-Galactosidase assay

HUVECs were irradiated at 10 Gy using a ^{137}Cs γ-ray source (Atomic Energy of Canada, Ltd, Canada) with a dose rate of 3.25 Gy/min. Irradiated HUVECs were subsequently treated with CA for 48 h. Prepared cells were fixed with 4% paraformaldehyde and subsequently stained using a β-galactosidase kit (Cell Signaling Technology, Danvers, MA, USA) according to the manufacturer's instructions.

Tube formation assay

Irradiated HUVECs were re-seeded onto Matrigel-coated transwell (Corning, NY, USA) followed by treatment with or without CA for 6 h. Angiogenic ability was observed under a light microscope and plotted using Image J.

Histological analysis of the intestine

Mouse small intestinal tissue samples were fixed with a 10% neutral buffered formalin solution, embedded in paraffin wax, and sectioned transversely at a thickness of 4 μm. The sections were then stained with hematoxylin and eosin (H&E). Evidence of intestinal mucosal injury was quantified (0 = none, 1 = mild, 2 = moderate, 3 = high) in H&E-stained sections of the ileum as a reference. The severity of radiation-induced enteritis was assessed by the degree of maintenance of the epithelial architecture, crypt damage, vascular enlargement, and infiltration of inflammatory cells in the lamina propria. This assessment is a modification of the histological score parameter used by Sung et al. [70]. To perform immunohistochemical analysis, slides were subjected to antigen retrieval and then treated with 0.3% hydrogen peroxide in methyl alcohol for 20 min to block endogenous peroxidase activity. After three washes in PBS, the sections were blocked with 10% normal goat serum (Vector ABC Elite kit; Vector Laboratories, Burlingame, CA, USA) and incubated with anti-Zo1 (#61-7300, Thermo Fisher Scientific, Waltham, MA, USA), anti- Dsg2 (#14415, Abcam), and anti-Cldn3 (#341700 Invitrogen, Carlsbad, CA, USA), anti-villin (#130751, Abcam), and anti-ki-67 (#DRM004, Acris, Herford, Germany) antibodies. After three washes in PBS, the sections were incubated with a horseradish peroxidase-conjugated secondary antibody (Dako, Carpinteria, CA, USA) for 60 min. The peroxidase reaction was developed using a diaminobenzidine substrate (Dako) prepared according to the manufacturer's instructions, and the slides were counterstained with hematoxylin.

Immunocytochemical staining

Caco-2 monolayers on coverslips were harvested and immunofluorescence analysis was performed. Cells were fixed with paraformaldehyde, blocked and permeabilized with 1% BSA and triton-X100 for 30 min at room temperature, and incubated with the primary antibodies specific for ZO1 and DSG2. Samples were incubated for 1 h at room temperature with the Alexa Fluor 488 (green)-conjugated anti-rabbit IgG and Alexa Fluor 592 (red)-conjugated anti-mouse IgG (Thermo Fisher Scientific) as secondary antibodies. After washing with DPBS, cells were count-stained with DAPI and mounted using Vectashield HardSet mounting medium. Fluorescence was examined using a confocal laser scanning microscope (LSM410; Carl Zeiss, Germany).

Bacterial translocation

To evaluate barrier function, treated mice were sacrificed, and the mesenteric lymph nodes were harvested under sterile conditions. The mesenteric lymph nodes were homogenized with sterile PBS and beads. The homogenized mixtures were centrifuged to remove cell debris and subsequently spread onto MacConkey agar (BD Biosciences). After incubation overnight, the colony-positive plates were counted. Data were graphed as the percentage of individual mice exhibiting colonies compared to individual control mice.

RNA extraction & qPCR

Total RNA of cells and in vivo samples was extracted using Tri-reagent (MRC, Cincinnati, OH, USA) according to the manufacturer's instructions. cDNA was synthesized using the AccuPower RT premix (Bioneer, Deajeon, Korea). Synthesized cDNA was amplified using a LightCycler 480 system (Roche, Basel, Switzerland) with specific primers. Expression levels of each gene were determined using the Delta-Delta-Ct (ddCt) method. The sequences of the primers were as follow: mouse *villin*, 5'-CACCTTTGGAAGCTTCTTCG – 3' (forward) and 5'-CTCTCGTTGCCTTGAACCTC-3'; mouse *tight junction protein 1* (*Tjp1)*, 5'-AGGACACCAAAGCATGTGAG-3' (forward) and 5'- GGCATTCCTGCTGGTTACA-3'; mouse *Dsg2*, 5'-GTAGGAGGTGCGATGCTCAA-3' (forward) and 5'- CATGCTGCCCTTTGGTAACG-3' (Reverse); mouse *Cldn3*, 5'-AAGCCGAATGGACAAAGAA-3' (forward) and 5'-CTGGCAAGTAGCTGCAGTG-3'; mouse *Gapdh*, 5'-TCCCTGGAGAAGAGCTATGA-3' (forward) and 5'-CGATAAAGGAAGGCTGGAA-3' (reverse); human *ZO1*, 5'-ATCCCTCAAGGAGCCATTC-3' (forward) and 5'- CACTTGTTTTGCCAGGTTTTA-3' (reverse); human *DSG2*, 5'-TGGACACCCAAACAGTGGCCCT-3' (forward) and 5'- CTCACTTTGTTGCAGCAGCACAC-3' (reverse); human *EGF*, 5'-GTGCAGCTTCAGGACCACAA-3' (forward) and 5'-AAATGCATGTGTCGAATATCTTGAG-3' (reverse); human *GAPDH*, 5'-GGACTCATGACCACAGTCCATGCC-3' (forward) and 5'-TCAGGGATGACCTTGCCCACAG-3' (reverse).

Western blot

Cell lysates were washed with PBS and lysed in cold RIPA supplemented with a cocktail of protease and phosphatase inhibitor (Roche) on ice. Protein concentrations were determined by a bicinchoninic acid (BCA) method using Pierce BCA protein Assay (Thermo Fisher Scientific). Equal quantity of samples mixed with sodium dodecyl sulfate (SDS)-containing sample buffer were boiled at 95°C for 5 min and separated by SDS-poly acrylamide gel electrophoresis. Proteins were transferred to polyvinylidene fluoride for immunoblotting (Bio-rad). The membrane was blocked with 5% skim milk in C. Primary antibodies diluted in tris-buffered saline and Tween 20 (TBS-T) were incubated overnight at 4°C. The following antibodies were used: anti-ZO1 (Thermo Fisher Scientific), anti-DSG2 (Abcam), and anti-β-Actin (Santa Cruz, CA, USA). Following overnight incubation, the membrane was washed and incubated with horseradish peroxidase-conjugated secondary antibodies for 1 h (Santa Cruz.) diluted in TBS-T. The membrane was washed, and proteins were detected using an enhanced chemiluminescence reagent (Pierce, Thermo Fisher Scientific).

TEER measurement

Caco-2 cells were seeded into the upper chamber of transwell (0.4-μm pore size, Corning) and cultured for 21 days to form epithelial monolayers. Caco-2 monolayers were exposed to radiation and followed by treatment with various experimental conditions. The EVOM system (WPI, Sarasota, FL, USA) was used to measure TEER values.

FITC-dextran flux measurement

Caco-2 cells were seeded into the upper chamber of transwell inserts (0.4-μm pore size, Corning) and cultured for 21 days. Caco-2 monolayers in the transwell were irradiated and incubated under various experimental conditions with 500 μg/ml of FITC-dextran (Sigma-Aldrich, St. Louis, MO, USA). Media in the lower-chamber were taken after 48 h and fluorescence was subsequently measured using a microplate fluorescence reader (excitation at 450 nm and emission at 520 nm). The flux of FITC into the lower-chamber was calculated as a percentage corresponding to control sample.

Dispase-based dissociation assay

To evaluate cell-cell adhesive strength, Caco-2 monolayers were washed and incubated in dispase II (2.4 U/ml, Roche) and collagenase type I (Gibco) for 30 min. To apply a mechanical stress, the Caco-2 monolayers were carefully subjected to pipetting with an automatic pipet. Released single cells were observed a digital camera.

Human protein cytokine array

HUVECs were irradiated and followed by CA or not in complete media. After 24 h, cells were washed once with PBS and exchanged to fresh serum-free medium. The CM of HUVECs were collected and spun down for removing cell debris. The CM was analyzed using the proteome profiler™ Human Cytokine Array Kit (R&D systems, Minneapolis, MN, USA) according to the manufacturer's instructions. Densitometry was performed with Image J (National Institute Health) to determine the relative abundance of cytokines in the CM.

ELISA

To quantify EGF, the CM was collected and spun down to remove cell debris. The CM was subjected to ELISA (R&D Systems) according to the manufacturer's instructions.

Neutralization of EGF

In the neutralizing experiment, each CM sample was prepared as described above and incubated with 100 ng/ml of anti-EGF (R&D systems) for 1 h to bind the antibody. Caco-2 monolayers were washed with PBS and pre-incubated medium was added. Cells were incubated for 48 h and subsequently analyzed by additional assays.

Statistical analysis

The in vitro data was plotted as mean ± standard deviation of the mean, and animal data are plotted as the mean ± standard error of the mean. Statistical analyses were performed using one-way analysis of variance (ANOVA) with the Tukey's multiple comparison test. Values of $P < 0.05$ were considered statistically significant.

Abbreviations

GI: Gastrointestinal; CA: *Centella asiatica*; CM: Conditioned media; EGF: Epidermal growth factor; HUVEC: Human umbilical vein endothelial cell; ZO1: Zonula occludens 1; DSG2: Desmoglein 2; CLDN3: Claudin 3; IR: Irradiation; TEER: Transepithelial electronical resistance; FITC: Fluorescein isothiocyanate; rEGF: Recombinant epidermal growth factor

Declarations

Ethics approval and consent to participate

All animal experiments were approved and performed in accordance with the guidelines of the Institutional Animal Care and Use Committee of the Korea Institute of Radiological & Medical Sciences (KIRAMS; kirams 2020-0010).

Consent for publication

All authors reached an agreement to publish this study in this journal.

Availability of data and materials

Data will be provided upon request.

Competing interests

There are no conflicts of interest to declare.

Funding

This research was supported by a grant from the Korea Institute of Radiological and Medical Sciences (KIRAMS), funded by the Ministry of Science and ICT (MSIT), Republic of Korea (grant numbers 50535-2021).

Authors' contributions

S.Y.K., S.S., W.I.J., S.P., S.S.J., and H.J. conceived and designed the experiments. S.Y.K., S.S., S.B.L., M-J.K., H.K., S-J.L., and H.J. performed the experiments. S.Y.K., S.S., and H.J. analyzed the data. S.Y.K. and H.J. wrote the manuscript. All authors agree to be accountable for the integrity and accuracy all aspects of the work.

Acknowledgements

Not applicable

Author details

[a]Laboratory of Radiation Exposure & Therapeutics, National Radiation Emergency Medical Center, Korea Institute of Radiological and Medical Sciences, Seoul 01812, Republic of Korea [b]Department of Surgery, Korea Institute of Radiological and Medical Sciences, Seoul 01812, Republic of Korea

References

1. Olcina MM, Giaccia AJ: Reducing radiation-induced gastrointestinal toxicity - the role of the PHD/HIF axis. *J Clin Invest* 2016, 126(10):3708-3715.

2. Shim S, Jang HS, Myung HW, Myung JK, Kang JK, Kim MJ, Lee SB, Jang WS, Lee SJ, Jin YW *et al*: Rebamipide ameliorates radiation-induced intestinal injury in a mouse model. *Toxicol Appl Pharmacol* 2017, 329:40-47.

3. Lu L, Li W, Chen L, Su Q, Wang Y, Guo Z, Lu Y, Liu B, Qin S: Radiation-induced intestinal damage: latest molecular and clinical developments. *Future Oncol* 2019, 15(35):4105-4118.

4. Cromer WE, Mathis JM, Granger DN, Chaitanya GV, Alexander JS: Role of the endothelium in inflammatory bowel diseases. *World J Gastroenterol* 2011, 17(5):578-593.

5. Wang J, Boerma M, Fu Q, Hauer-Jensen M: Significance of endothelial dysfunction in the pathogenesis of early and delayed radiation enteropathy. *World J Gastroenterol* 2007, 13(22):3047-3055.

6. Lee CL, Daniel AR, Holbrook M, Brownstein J, Silva Campos LD, Hasapis S, Ma Y, Borst LB, Badea CT, Kirsch DG: Sensitization of Vascular Endothelial Cells to Ionizing Radiation Promotes the Development of Delayed Intestinal Injury in Mice. *Radiation research* 2019, 192(3):258-266.

7. Korpela E, Liu SK: Endothelial perturbations and therapeutic strategies in normal tissue radiation damage. *Radiat Oncol* 2014, 9:266.

8. Okunieff P, Mester M, Wang J, Maddox T, Gong X, Tang D, Coffee M, Ding I: In vivo radioprotective effects of angiogenic growth factors on the small bowel of C3H mice. *Radiation research* 1998, 150(2):204-211.

9. Fung KYY, Fairn GD, Lee WL: Transcellular vesicular transport in epithelial and endothelial cells: Challenges and opportunities. *Traffic* 2018, 19(1):5-18.

10. Blume ED, Taylor CT, Lennon PF, Stahl GL, Colgan SP: Activated endothelial cells elicit paracrine induction of epithelial chloride secretion. 6-Keto-PGF1alpha is an epithelial secretagogue. *J Clin Invest* 1998, 102(6):1161-1172.

11. Wang P, Luo R, Zhang M, Wang Y, Song T, Tao T, Li Z, Jin L, Zheng H, Chen W *et al*: A cross-talk between epithelium and endothelium mediates human alveolar-capillary injury during SARS-CoV-2 infection. *Cell Death Dis* 2020, 11(12):1042.

12. Chowdhury F, Howat WJ, Phillips GJ, Lackie PM: Interactions between endothelial cells and epithelial cells in a combined cell model of airway mucosa: effects on tight junction permeability. *Exp Lung Res* 2010, 36(1):1-11.

13. Caccia D, Zanetti Domingues L, Miccichè F, De Bortoli M, Carniti C, Mondellini P, Bongarzone I: Secretome compartment is a valuable source of biomarkers for cancer-relevant pathways. *J Proteome Res* 2011, 10(9):4196-4207.

14. Pocock JM, Storisteanu DML, Reeves MB, Juss JK, Wills MR, Cowburn AS, Chilvers ER: Human Cytomegalovirus Delays Neutrophil Apoptosis and Stimulates the Release of a Prosurvival Secretome. *Front Immunol* 2017, 8:1185.

15. Hendrata M, Sudiono J: A Computational Model for Investigating Tumor Apoptosis Induced by Mesenchymal Stem Cell-Derived Secretome. *Comput Math Methods Med* 2016, 2016:4910603.

16. Groschwitz KR, Hogan SP: Intestinal barrier function: molecular regulation and disease pathogenesis. *J Allergy Clin Immunol* 2009, 124(1):3-20; quiz 21-22.

17. Capaldo CT, Farkas AE, Nusrat A: Epithelial adhesive junctions. *F1000Prime Rep* 2014, 6:1.

18. Ivanov AI, Naydenov NG: Dynamics and regulation of epithelial adherens junctions: recent discoveries and controversies. *Int Rev Cell Mol Biol* 2013, 303:27-99.

19. Van Itallie CM, Anderson JM: Architecture of tight junctions and principles of molecular composition. *Semin Cell Dev Biol* 2014, 36:157-165.

20. Khare V, Krnjic A, Frick A, Gmainer C, Asboth M, Jimenez K, Lang M, Baumgartner M, Evstatiev R, Gasche C: Mesalamine and azathioprine modulate junctional complexes and restore epithelial barrier function in intestinal inflammation. *Sci Rep* 2019, 9(1):2842.

21. Ungewiß H, Vielmuth F, Suzuki ST, Maiser A, Harz H, Leonhardt H, Kugelmann D, Schlegel N, Waschke J: Desmoglein 2 regulates the intestinal epithelial barrier via p38 mitogen-activated protein kinase. *Sci Rep* 2017, 7(1):6329.

22. Gross A, Pack LAP, Schacht GM, Kant S, Ungewiss H, Meir M, Schlegel N, Preisinger C, Boor P, Guldiken N *et al*: Desmoglein 2, but not desmocollin 2, protects intestinal epithelia from injury. *Mucosal Immunol* 2018, 11(6):1630-1639.

23. Somboonwong J, Kankaisre M, Tantisira B, Tantisira MH: Wound healing activities of different extracts of Centella asiatica in incision and burn wound models: an experimental animal study. *BMC Complement Altern Med* 2012, 12:103.

24. Cheng CL, Koo MW: Effects of Centella asiatica on ethanol induced gastric mucosal lesions in rats. *Life Sci* 2000, 67(21):2647-2653.

25. Shukla A, Rasik AM, Jain GK, Shankar R, Kulshrestha DK, Dhawan BN: In vitro and in vivo wound healing activity of asiaticoside isolated from Centella asiatica. *J Ethnopharmacol* 1999, 65(1):1-11.

26. Brinkhaus B, Lindner M, Schuppan D, Hahn EG: Chemical, pharmacological and clinical profile of the East Asian medical plant Centella asiatica. *Phytomedicine* 2000, 7(5):427-448.

27. Ponnusamy K, Mohan M, Nagaraja HS: Protective antioxidant effect of Centella asiatica bioflavonoids on lead acetate induced neurotoxicity. *Med J Malaysia* 2008, 63 Suppl A:102.

28. Buranasudja V, Rani D, Malla A, Kobtrakul K, Vimolmangkang S: Insights into antioxidant activities and anti-skin-aging potential of callus extract from Centella asiatica (L.). *Sci Rep* 2021, 11(1):13459.

29. Zhang Z, Cai P, Zhou J, Liu M, Jiang X: Effects of asiaticoside on human umbilical vein endothelial cell apoptosis induced by Aβ1-42. *Int J Clin Exp Med* 2015, 8(9):15828-15833.

30. Bian D, Liu M, Li Y, Xia Y, Gong Z, Dai Y: Madecassoside, a triterpenoid saponin isolated from Centella asiatica herbs, protects endothelial cells against oxidative stress. *J Biochem Mol Toxicol* 2012, 26(10):399-406.

31. Fong LY, Ng CT, Yong YK, Hakim MN, Ahmad Z: Asiatic acid stabilizes cytoskeletal proteins and prevents TNF-α-induced disorganization of cell-cell junctions in human aortic endothelial cells. *Vascul Pharmacol* 2019, 117:15-26.

32. Chen Z, Cao K, Xia Y, Li Y, Hou Y, Wang L, Li L, Chang L, Li W: Cellular senescence in ionizing radiation (Review). *Oncol Rep* 2019, 42(3):883-894.

33. Odenwald MA, Turner JR: The intestinal epithelial barrier: a therapeutic target? *Nat Rev Gastroenterol Hepatol* 2017, 14(1):9-21.

34. Hollander D: Crohn's disease--a permeability disorder of the tight junction? *Gut* 1988, 29(12):1621-1624.

35. Schmitz H, Barmeyer C, Fromm M, Runkel N, Foss HD, Bentzel CJ, Riecken EO, Schulzke JD: Altered tight junction structure contributes to the impaired epithelial barrier function in ulcerative colitis. *Gastroenterology* 1999, 116(2):301-309.

36. Blair SA, Kane SV, Clayburgh DR, Turner JR: Epithelial myosin light chain kinase expression and activity are upregulated in inflammatory bowel disease. *Lab Invest* 2006, 86(2):191-201.

37. Cai Y, Wang W, Liang H, Sun L, Teitelbaum DH, Yang H: Keratinocyte growth factor pretreatment prevents radiation-induced intestinal damage in a mouse model. *Scand J Gastroenterol* 2013, 48(4):419-426.

38. Tessner TG, Muhale F, Riehl TE, Anant S, Stenson WF: Prostaglandin E2 reduces radiation-induced epithelial apoptosis through a mechanism involving AKT activation and bax translocation. *J Clin Invest* 2004, 114(11):1676-1685.

39. Orazi A, Du X, Yang Z, Kashai M, Williams DA: Interleukin-11 prevents apoptosis and accelerates recovery of small intestinal mucosa in mice treated with combined chemotherapy and radiation. *Lab Invest* 1996, 75(1):33-42.

40. Darling NJ, Mobbs CL, González-Hau AL, Freer M, Przyborski S: Bioengineering Novel in vitro Co-culture Models That Represent the Human Intestinal Mucosa With Improved Caco-2 Structure and Barrier Function. *Front Bioeng Biotechnol* 2020, 8:992.

41. Sambuy Y, De Angelis I, Ranaldi G, Scarino ML, Stammati A, Zucco F: The Caco-2 cell line as a model of the intestinal barrier: influence of cell and culture-related factors on Caco-2 cell functional characteristics. *Cell Biol Toxicol* 2005, 21(1):1-26.

42. Alwjwaj M, Kadir RRA, Bayraktutan U: The secretome of endothelial progenitor cells: a potential therapeutic strategy for ischemic stroke. *Neural Regen Res* 2021, 16(8):1483-1489.

43. Ishikawa S, Cepinskas G, Specian RD, Itoh M, Kvietys PR: Epidermal growth factor attenuates jejunal mucosal injury induced by oleic acid: role of mucus. *Am J Physiol* 1994, 267(6 Pt 1):G1067-1077.

44. Rao R, Porreca F: Epidermal growth factor protects mouse ileal mucosa from Triton X-100-induced injury. *Eur J Pharmacol* 1996, 303(3):209-212.

45. Vinter-Jensen L: Pharmacological effects of epidermal growth factor (EGF) with focus on the urinary and gastrointestinal tracts. *APMIS Suppl* 1999, 93:1-42.

46. Murphy MS: Growth factors and the gastrointestinal tract. *Nutrition* 1998, 14(10):771-774.

47. Nair RR, Warner BB, Warner BW: Role of epidermal growth factor and other growth factors in the prevention of necrotizing enterocolitis. *Semin Perinatol* 2008, 32(2):107-113.

48. Tang X, Liu H, Yang S, Li Z, Zhong J, Fang R: Epidermal Growth Factor and Intestinal Barrier Function. *Mediators Inflamm* 2016, 2016:1927348.

49. Sun B, Wu L, Wu Y, Zhang C, Qin L, Hayashi M, Kudo M, Gao M, Liu T: Therapeutic Potential of Centella asiatica and Its Triterpenes: A Review. *Front Pharmacol* 2020, 11:568032.

50. Sh Ahmed A, Taher M, Mandal UK, Jaffri JM, Susanti D, Mahmood S, Zakaria ZA: Pharmacological properties of Centella asiatica hydrogel in accelerating wound healing in rabbits. *BMC Complement Altern Med* 2019, 19(1):213.

51. Moghaddam SS, Jaafar H, Ibrahim R, Rahmat A, Aziz MA, Philip E: Effects of acute gamma irradiation on physiological traits and flavonoid accumulation of Centella asiatica. *Molecules* 2011, 16(6):4994-5007.

52. Sharma J, Sharma R: Radioprotection of Swiss albino mouse by Centella asiatica extract. *Phytother Res* 2002, 16(8):785-786.

53. Shobi V, Goel HC: Protection against radiation-induced conditioned taste aversion by Centella asiatica. *Physiol Behav* 2001, 73(1-2):19-23.

54. Onyiah JC, Colgan SP: Cytokine responses and epithelial function in the intestinal mucosa. *Cell Mol Life Sci* 2016, 73(22):4203-4212.

55. Blume C, Reale R, Held M, Loxham M, Millar TM, Collins JE, Swindle EJ, Morgan H, Davies DE: Cellular crosstalk between airway epithelial and endothelial cells regulates barrier functions during exposure to double-stranded RNA. *Immun Inflamm Dis* 2017, 5(1):45-56.

56. Carpenter G, Cohen S: Epidermal growth factor. *Annu Rev Biochem* 1979, 48:193-216.

57. Hackel PO, Zwick E, Prenzel N, Ullrich A: Epidermal growth factor receptors: critical mediators of multiple receptor pathways. *Curr Opin Cell Biol* 1999, 11(2):184-189.

58. Rao RK: Biologically active peptides in the gastrointestinal lumen. *Life Sci* 1991, 48(18):1685-1704.

59. Bhora FY, Dunkin BJ, Batzri S, Aly HM, Bass BL, Sidawy AN, Harmon JW: Effect of growth factors on cell proliferation and epithelialization in human skin. *J Surg Res* 1995, 59(2):236-244.

60. Fatimah SS, Tan GC, Chua KH, Tan AE, Hayati AR: Effects of epidermal growth factor on the proliferation and cell cycle regulation of cultured human amnion epithelial cells. *J Biosci Bioeng* 2012, 114(2):220-227.

61. Doan PL, Himburg HA, Helms K, Russell JL, Fixsen E, Quarmyne M, Harris JR, Deoliviera D, Sullivan JM, Chao NJ *et al*: Epidermal growth factor regulates hematopoietic regeneration after radiation injury. *Nat Med* 2013, 19(3):295-304.

62. Oh H, Seong J, Kim W, Park S, Koom WS, Cho NH, Song M: Recombinant human epidermal growth factor (rhEGF) protects radiation-induced intestine injury in murine system. *J Radiat Res* 2010, 51(5):535-541.

63. Lee KK, Jo HJ, Hong JP, Lee SW, Sohn JS, Moon SY, Yang SH, Shim H, Lee SH, Ryu SH *et al*: Recombinant human epidermal growth factor accelerates recovery of mouse small intestinal mucosa after radiation damage. *Int J Radiat Oncol Biol Phys* 2008, 71(4):1230-1235.

64. Buckley A, Turner JR: Cell Biology of Tight Junction Barrier Regulation and Mucosal Disease. *Cold Spring Harb Perspect Biol* 2018, 10(1).

65. Shukla PK, Gangwar R, Manda B, Meena AS, Yadav N, Szabo E, Balogh A, Lee SC, Tigyi G, Rao R: Rapid disruption of intestinal epithelial tight junction and barrier dysfunction by ionizing radiation in mouse colon in vivo: protection by N-acetyl-l-cysteine. *Am J Physiol Gastrointest Liver Physiol* 2016, 310(9):G705-715.

66. Poritz LS, Garver KI, Green C, Fitzpatrick L, Ruggiero F, Koltun WA: Loss of the tight junction protein ZO-1 in dextran sulfate sodium induced colitis. *J Surg Res* 2007, 140(1):12-19.

67. Yoseph BP, Klingensmith NJ, Liang Z, Breed ER, Burd EM, Mittal R, Dominguez JA, Petrie B, Ford ML, Coopersmith CM: Mechanisms of Intestinal Barrier Dysfunction in Sepsis. *Shock* 2016, 46(1):52-59.

68. Kuo W-T, Zuo L, Turner J: THE TIGHT JUNCTION PROTEIN ZO-1 REGULATES MITOTIC SPINDLE ORIENTATION TO ENABLE EFFICIENT MUCOSAL REPAIR. *Inflammatory Bowel Diseases* 2021, 27(Supplement_1):S28-S28.

69. Schlegel N, Meir M, Heupel WM, Holthöfer B, Leube RE, Waschke J: Desmoglein 2-mediated adhesion is required for intestinal epithelial barrier integrity. *Am J Physiol Gastrointest Liver Physiol* 2010, 298(5):G774-783.

70. Sung J, Sodhi CP, Voltaggio L, Hou X, Jia H, Zhou Q, Čiháková D, Hackam DJ: The recruitment of extra-intestinal cells to the injured mucosa promotes healing in radiation enteritis and chemical colitis in a mouse parabiosis model. *Mucosal Immunol* 2019, 12(2):503-517.

Figures

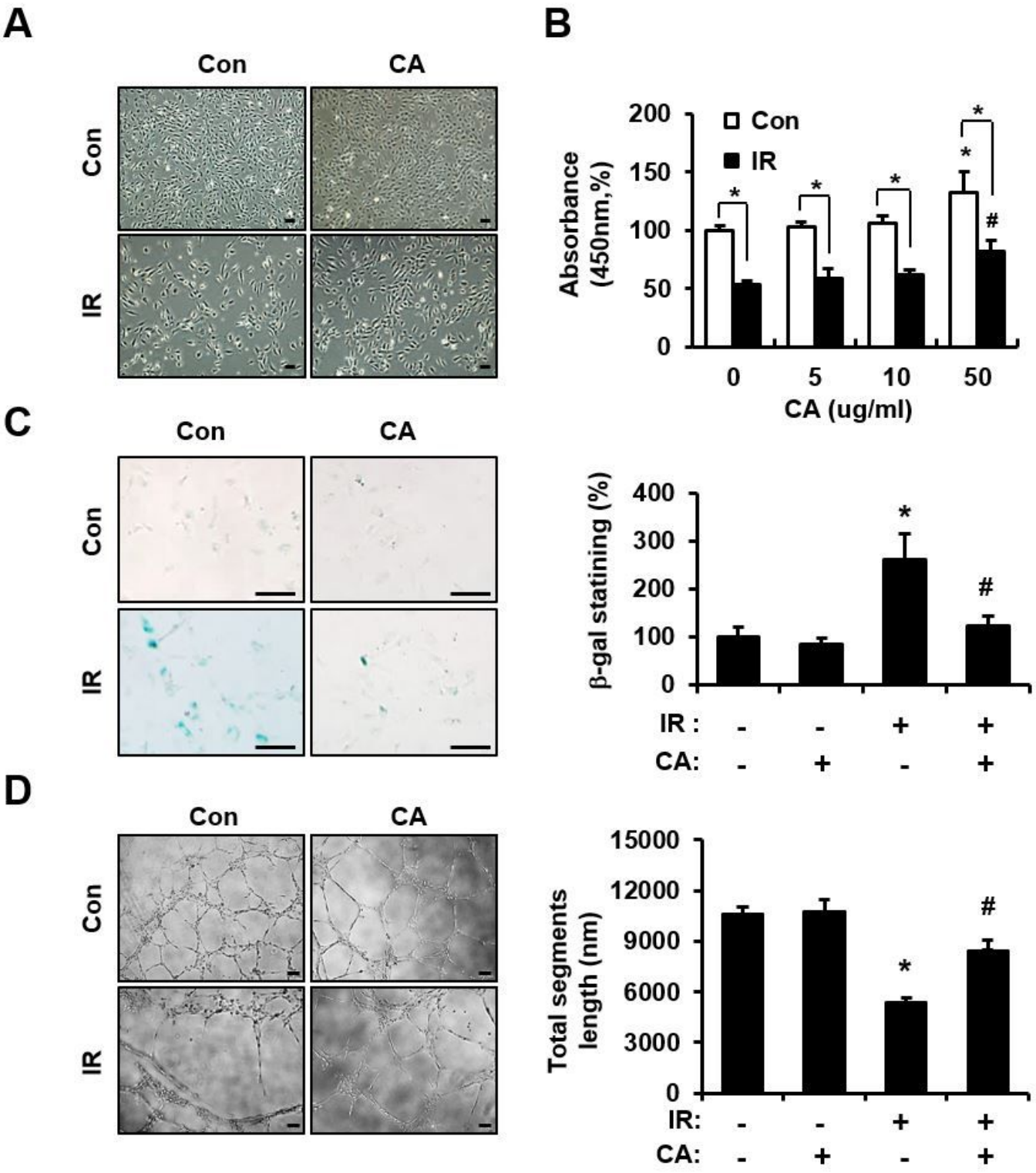

Figure 1

Centella asiatica mitigates radiation-induced endothelial dysfunction. (A) Observation of HUVECs after irradiation and treatment with Centella asiatica (CA). Representative images were taken using a phase-contrast microscope. (B) Determination of proliferation of HUVECs. HUVECs were irradiated and treated with or without CA. The effect of CA on HUVEC proliferation was assessed by CCK-8 assay. Bars represent the percentage of proliferating cells normalized to that of the corresponding control. (C)

Determination of senescent activity of CA. HUVECs were irradiated and treated with or without CA. Senescent HUVECs were quantified by a β-galactosidase assay. Senescent HUVECs were quantified and plotted as a bar graph (right). (D) Determination of angiogenic activity. HUVECs were re-seeded onto Matrigel-coated wells in the presence or absence of CA. Total segments length per five fields were quantified and plotted as a bar graph (right). Data are presented as the means ± standard deviation of triplicate experiments. Images are representative of 3 independent experiments. *P < 0.05 vs. negative control (Con). #P < 0.05 vs. irradiated control (IR). Scale bars represent 100 μm.

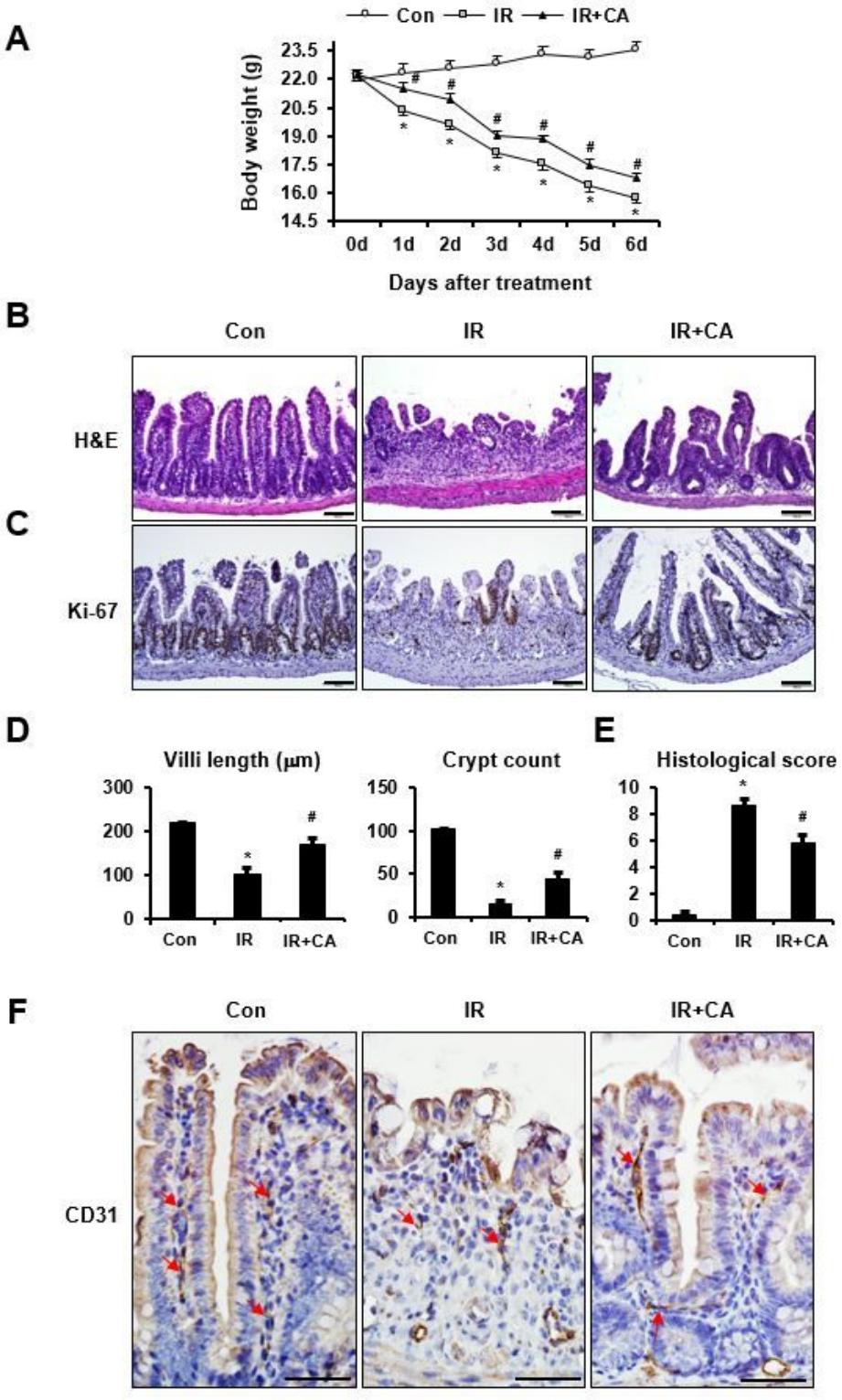

Figure 2

Centella asiatica alleviates radiation-induced enteropathy in mouse model. (A) Body weights of control (Con), irradiated (IR), and Centella asiatica (CA)-treated irradiated mice (IR+CA). (B) Hematoxylin and eosin (H&E) staining was performed using small intestine of Con, IR, and IR+CA groups. (C) Representative images of the small intestine stained with Ki-67 showing proliferation. Scale bars represent 100 μm. (D) The length of villi and crypts in the small intestine were quantified. (E) Histological scoring was assessed based on the degree of epithelial architecture maintenance, crypt disruption, vascular enlargement, and infiltration of inflammatory cells in the lamina propria of the ileum of Con, IR, and IR+CA mice groups (0 = none, 1 = mild, 2 = moderate, 3 = high). (F) Representative images of the small intestine stained with CD31 showing the positive endothelial cells. Red arrows indicate the positive endothelial cells. Scale bars represent 50 μm. Data are presented as the mean ± standard error of the mean; n = 5 mice per group. *P < 0.05 compared to the Con group; #P < 0.05 compared to the IR group.

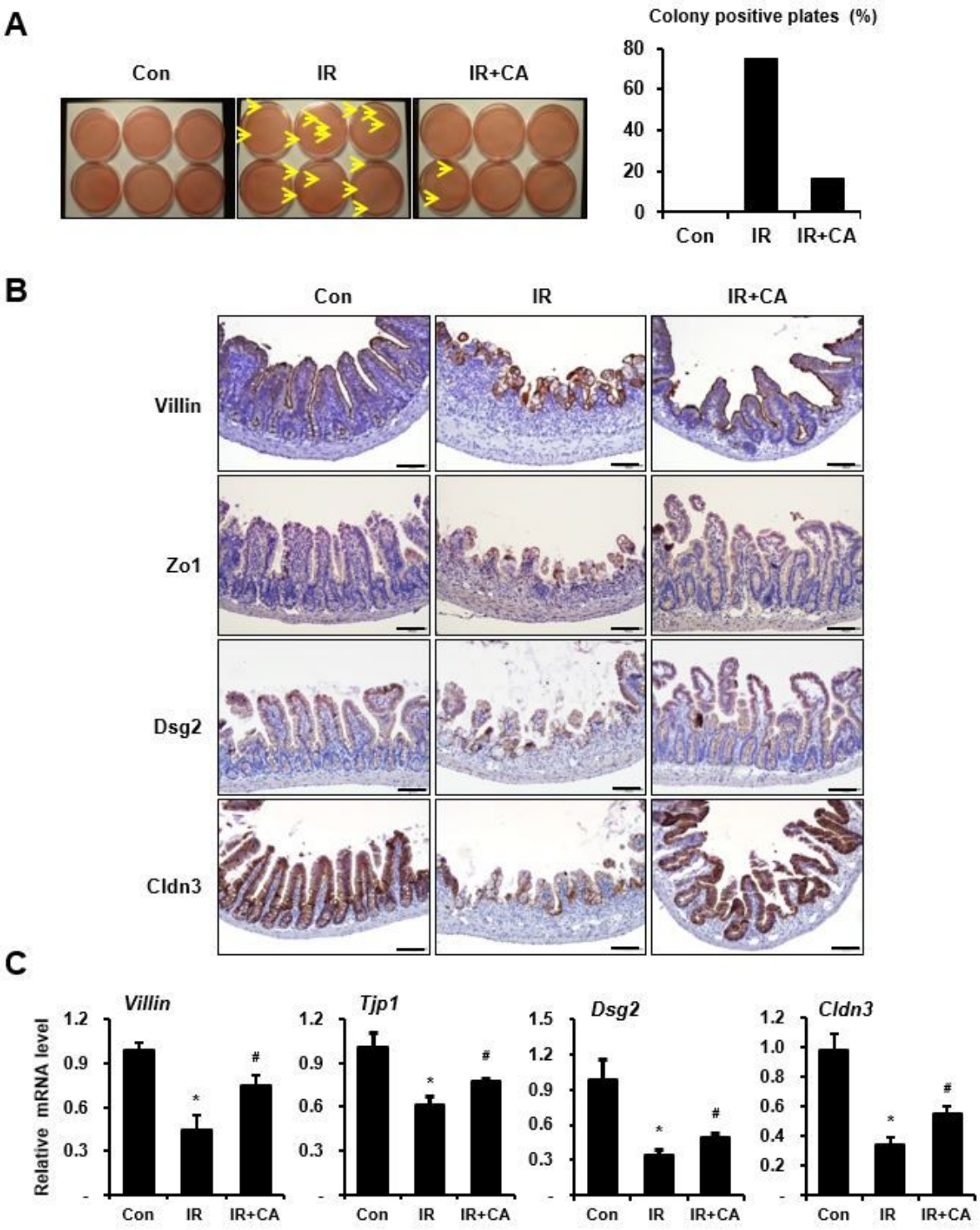

Figure 3

Centella asiatica ameliorates radiation-induced intestinal barrier dysfunction in vivo. (A) The bacterial colonies from mesenteric lymph node of control (Con), irradiated (IR), and Centella asiatica (CA)-treated IR group (IR+CA) were quantified. The graph is depicted as the percentage of individual mice exhibiting colonies in the group. n = 5 mice per group. (B) Representative images of small intestine stained with villin, zonula occludens 1 (Zo1), desmoglein 2 (Dsg2), and claudin 3 (Cldn3). (C) qRT-PCR analysis

demonstrating the mRNA levels of Villin, Tjp1, Dsg2, and Cldn3 in small intestine of each group. Data are presented as the mean ± standard error of the mean; n = 5 mice per group. *P < 0.05 compared to the Con group; #P < 0.05 compared to the IR group. Scale bars represent 100 μm.

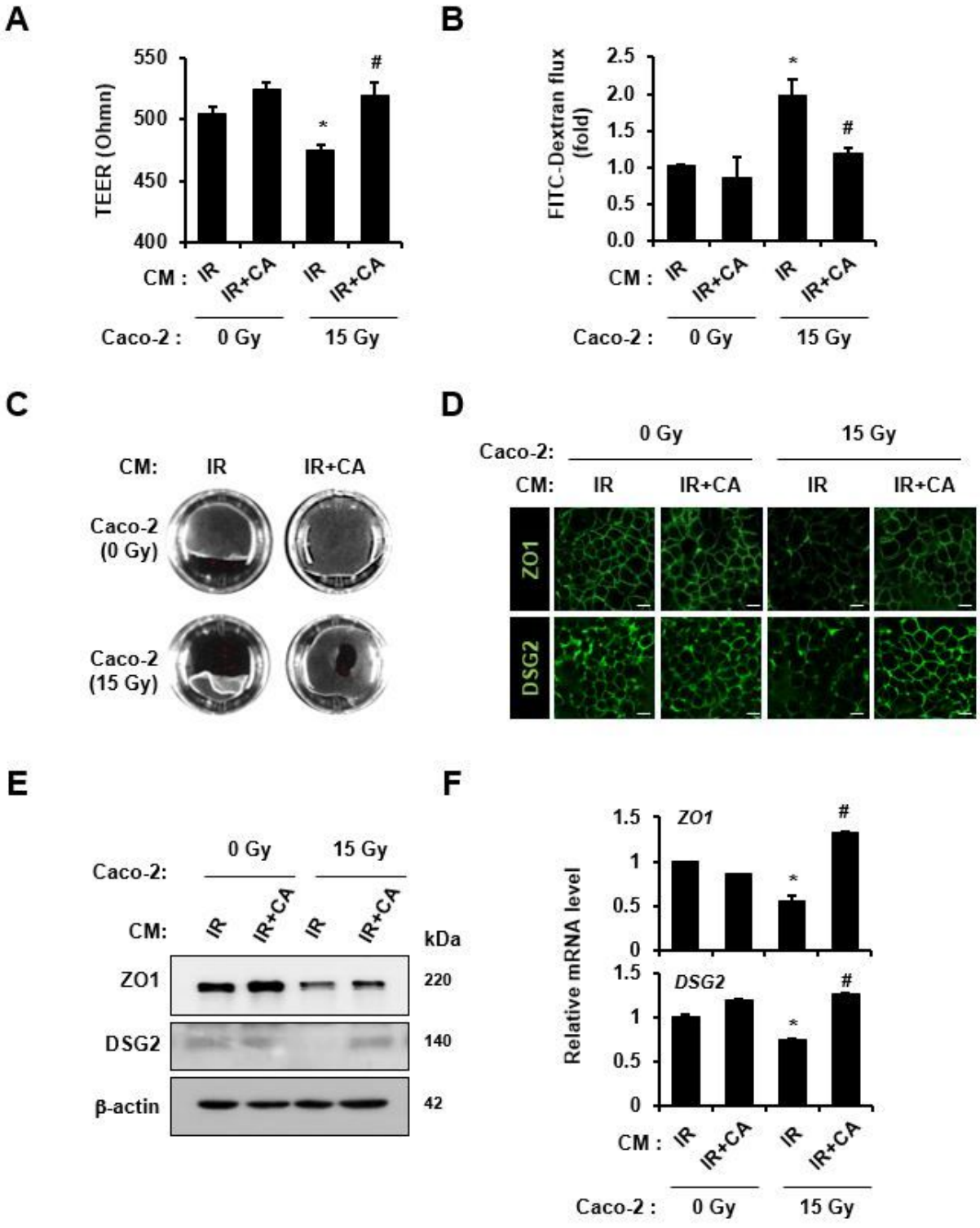

Figure 4

The conditioned medium of Centella asiatica-treated HUVECs exerts recovery effect of radiation-induced epithelium dysfunction. (A) The transepithelial electronical resistance (TEER) value of Caco-2 monolayers

on Transwell inserts was determined using the EVOM system. The TEER value of each group is shown in a bar graph. The groups are as follows; Conditioned medium (CM) of irradiated (IR)-HUVECs treating non-irradiated Caco-2 monolayers, CM of CA (Centella asiatica)-treated irradiated (IR+CA)-HUVECS treating non-irradiated Caco-2 monolayers, CM of IR treating irradiated Caco-2 monolayers, and CM of IR+CA treating irradiated Caco-2 monolayers. (B) The flux of FITC-dextran (4 kDa) in the lower-chamber was measured using a microplate fluorescence reader (excitation at 450 nm and emission at 520 nm). The bar graph is shown as a fold of flux of fluorescence normalized to CM of IR treating non-irradiated Caco-2 monolayers. (C) Dispase-based dissociation activity of each Caco-2 monolayer was determined. Treated Caco-2 monolayers were incubated in dispase II (2.4 U/ml) and collagenase type I for 30 min. After applying mechanical stress, the fragmentation of Caco-2 monolayers was observed using a digital camera. (D) The intensity of zonula occludens 1 (ZO1) and desmoglein 2 (DSG2) on intercellular junction of Caco-2 monolayers was assessed by confocal staining. Caco-2 monolayers on coverslips were stained with primary antibody against to ZO1 and DSG2. After mounting the samples, fluorescence was examined using a confocal laser scanning microscope (Carl Zeiss). (E) Protein levels of ZO1 and DSG2 were assessed by western blot analysis. (F) mRNA levels of ZO1 and DSG2 were assessed by qRT-PCR. Data are presented as the mean ± standard deviation of the mean; n = 3 per group. *P < 0.05 compared to CM of IR treating non-irradiated Caco-2 monolayers; #P < 0.05 compared to the CM of IR treating irradiated Caco-2 monolayers. Scale bars represent 10 μm.

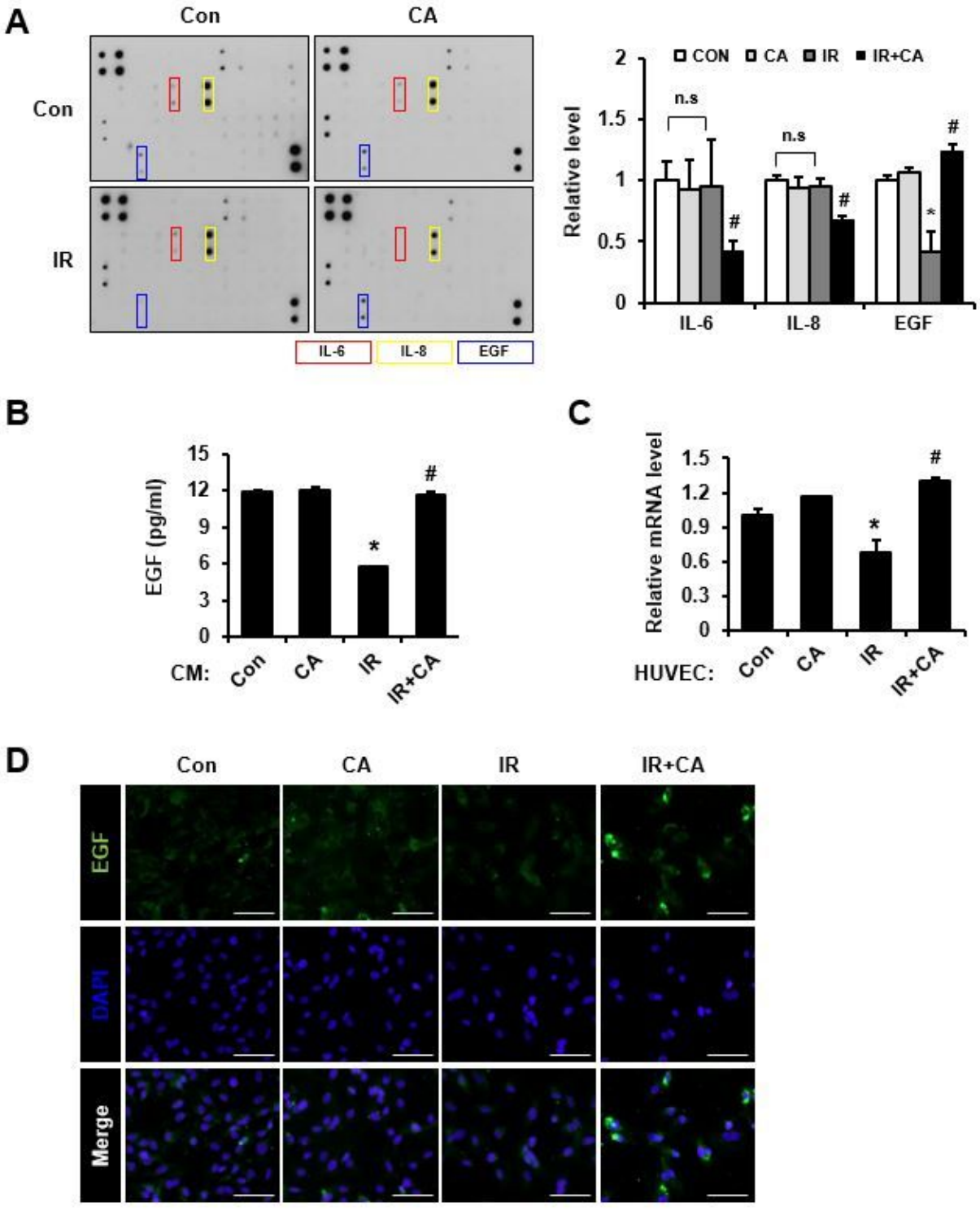

Figure 5

Epidermal growth factor is a key regulator of restoration of radiation-induced epithelial barrier dysfunction. (A) The cytokine array was performed using the conditioned media of control (Con), irradiated (IR), CA-treated HUVECs (CA), and CA-treated irradiated HUVECs (IR+CA). The bar graph is shown as relative folds of interleukin (IL)-6, IL-8, and EGF. (B) Secretion of epidermal growth factor (EGF) was quantified by performing ELISA. (C) The mRNA level of EGF was determined by qRT-PCR. (D) The

EGF-positive cells were observed by confocal laser scanning microscope. Data are presented as the mean ± standard deviation of the mean; n = 3, *P < 0.05 compared to the Con group; #P < 0.05 compared to the IR group. Scale bars represent 50 μm.

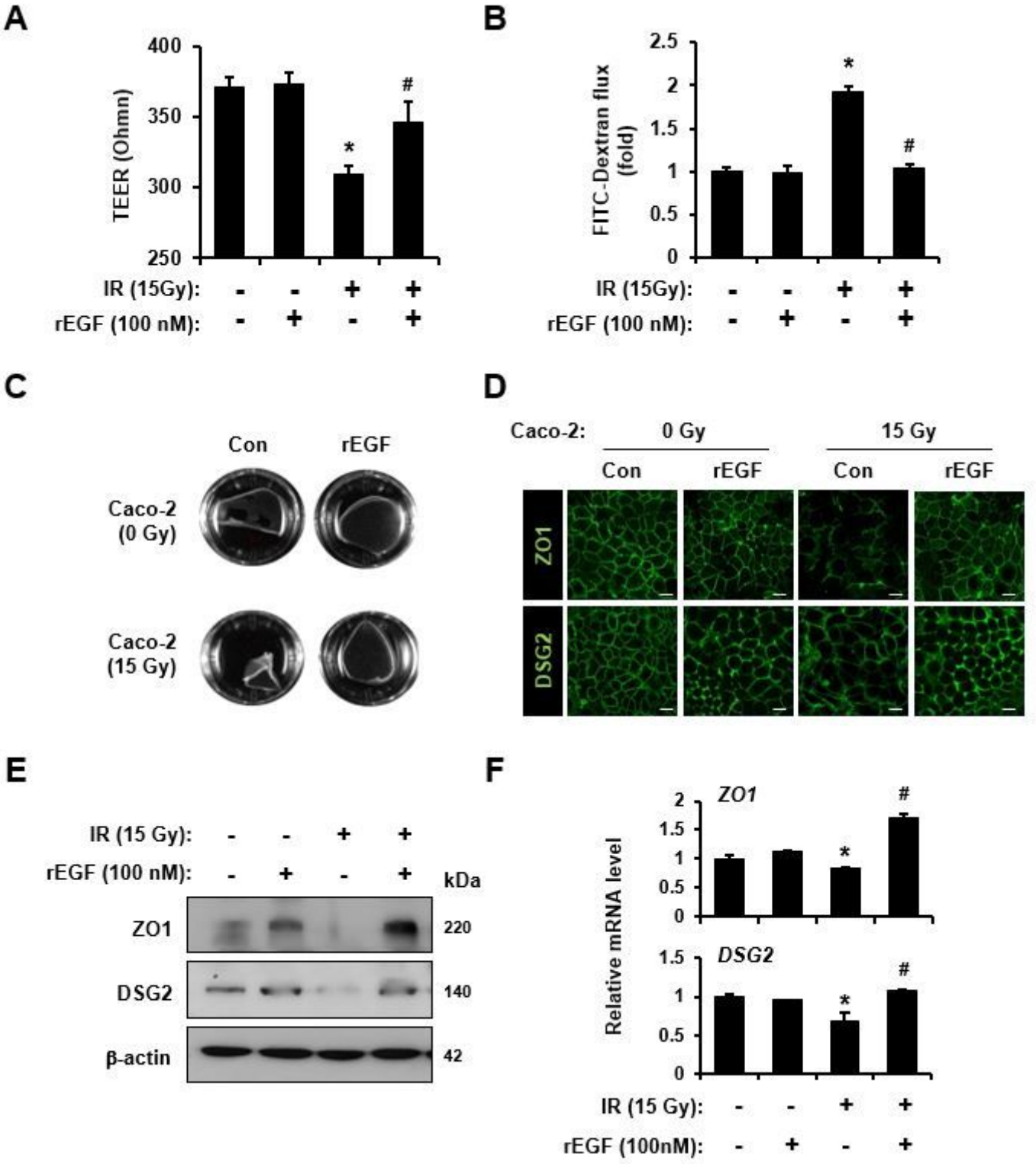

Figure 6

Epidermal growth factor relieves radiation-induced epithelium barrier dysfunction. (A) Transepithelial electronical resistance (TEER) values of Caco-2 monolayers were determined after treatment with

recombinant epidermal growth factor (rEGF; 100 nM). (B) The flux of FITC-dextran was measured using a microplate fluorescence reader (excitation at 450 nm and emission at 520 nm). The graph is shown as a fold of fluorescence normalized to control group. (C) The activity of dispase-based dissociation in Caco-2 monolayers with or without rEGF was observed. (D) The zonula occludens 1 (ZO1) and desmoglein 2 (DSG2) intensities on intercellular junction of Caco-2 monolayers were observed using a confocal laser scanning microscope. (E) Protein levels of ZO1 and DSG2 were determined by western blot analysis. (F) mRNA levels of ZO1 and DSG2 were measured by qRT-PCR. Data are presented as the mean ± standard deviation of the mean; n = 3, *P < 0.05 compared to the Con group; #P < 0.05 compared to the IR group. Scale bars represent 10 μm.

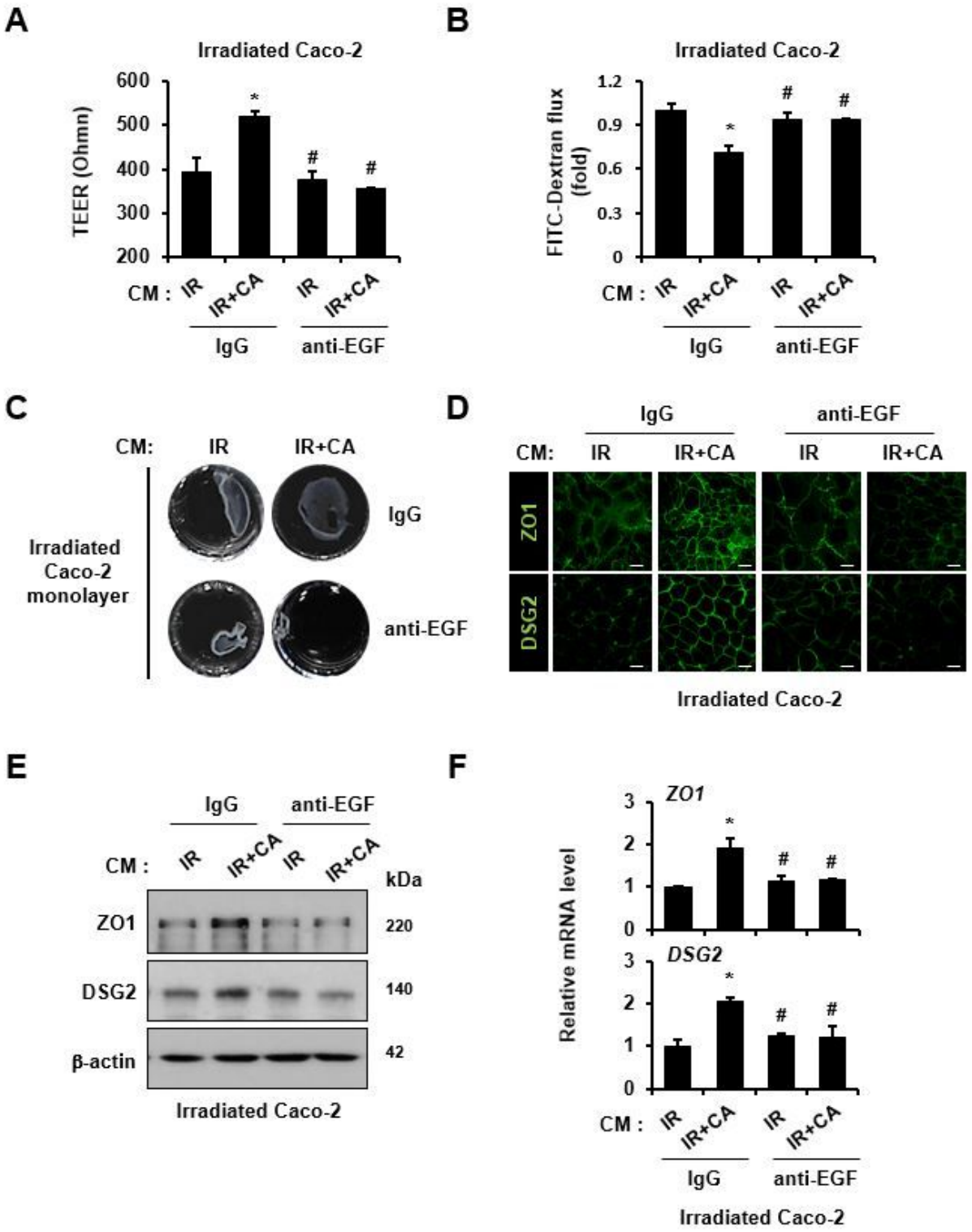

Figure 7

Epidermal growth factor driven by Centella asiatica-treated HUVECs regulates the radiation-induced epithelial cell barrier dysfunction. (A) Transepithelial electronical resistance (TEER) value of irradiated Caco-2 monolayers on transwells was determined after treatment with CM of irradiated (IR) HUVECs or CA-treated IR in presence of neutralizing antibody to EGF (anti-EGF, 100 ng/ml). The bar graph Is shown as TEER value of each group. (B) The flux of FITC-dextran (4 kDa) in lower chambers was measured

using a microplate fluorescence reader (excitation at 450 nm and emission at 520 nm). The bar graph is shown as a fold of flux of fluorescence normalized to irradiated Caco-2 monolayers treated with CM of IR. (C) Dispase-based dissociation activity of each irradiated Caco-2 monolayer was determined. Prepared irradiated Caco-2 monolayers were incubated in dispase II (2.4 U/ml) and collagenase type I for 30 min. After applying mechanical stress, the fragmentation of Caco-2 monolayers was observed using a digital camera. (D) The intensity of zonula occludens 1 (ZO1) and desmoglein 2 (DSG2) on the intercellular junction of irradiated Caco-2 monolayers was assessed by confocal staining. Caco-2 monolayers on coverslips were irradiated and treated with the CM of IR and IR+CA in the presence of anti-EGF. Caco-2 monolayers were stained with primary antibody against ZO1 and DSG2. After mounting the samples, fluorescence was examined using a confocal laser scanning microscope (Carl Zeiss). (E) Protein levels of ZO1 and DSG2 were assessed by western blot analysis. (F) mRNA levels of ZO1 and DSG2 were assessed by qRT-PCR. Data are presented as the mean ± standard error of the mean; n = 3 per group. *P < 0.05 compared to the CM of IR-treated irradiated Caco-2 monolayers; #P < 0.05 compared to the CM of IR+CA treated irradiated Caco-2 monolayers. Scale bars represent 10 μm.

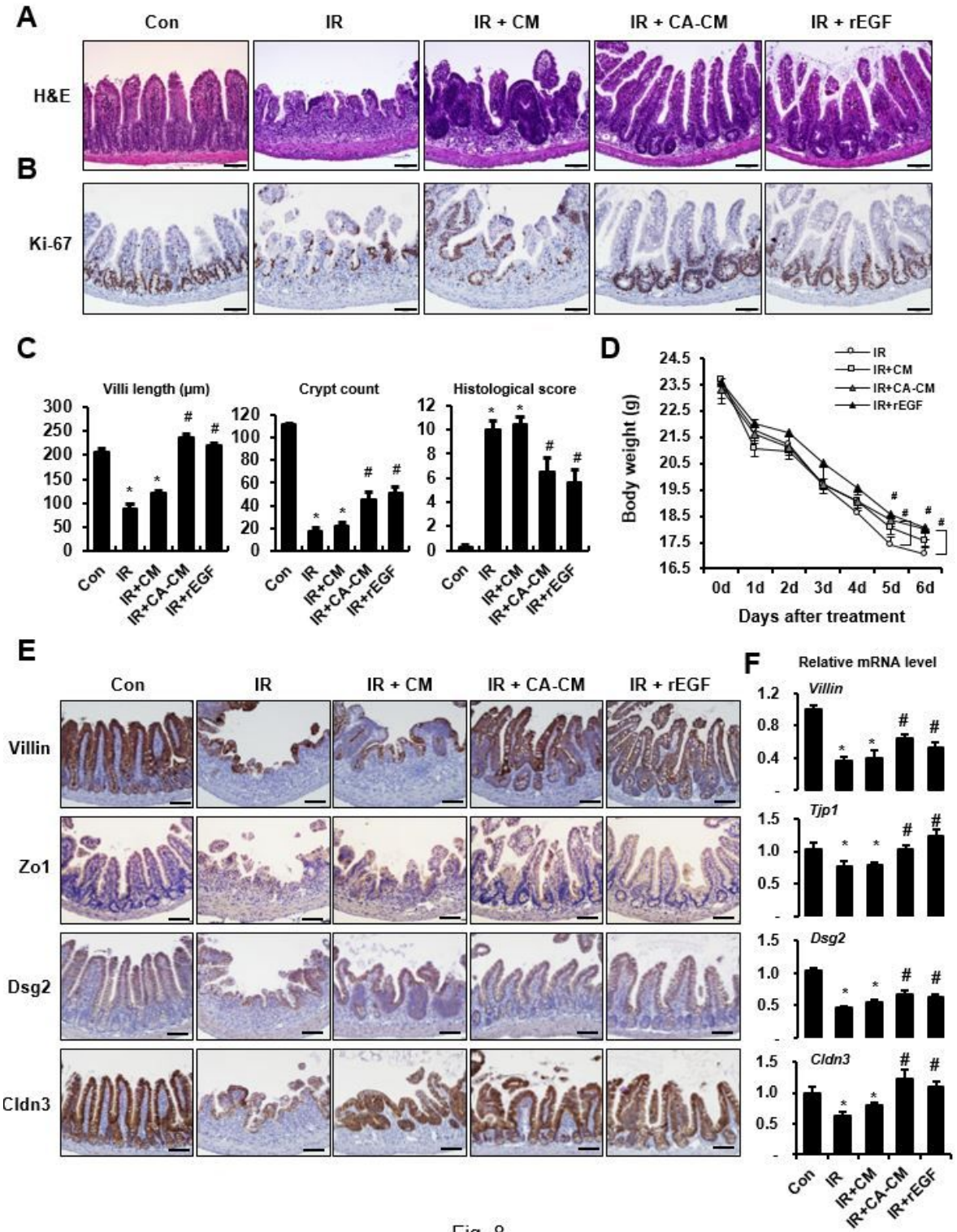

Fig. 8.

Figure 8

The conditioned media of Centella asiatica-treated HUVECs alleviates radiation-induced enteropathy and barrier dysfunction in vivo. Mouse groups are as follow; Control (Con), irradiated (IR), irradiated mouse administrated with the conditioned media (CM) of irradiated HUVECs (IR + CM), CM of Centella asiatica (CA)-treated irradiated HUVECs (IR + CA-CM), and recombinant EGF (IR + rEGF). (A) Hematoxylin and eosin staining of mouse intestinal tissue sections was performed in each group. (B) Proliferation was

assessed by staining intestinal sections with ki-67. (C) The lengths of villi and crypts in the intestinal sections were quantified. Histological scoring was assessed based on the degree of epithelial architecture maintenance, crypt disruption, vascular enlargement, and infiltration of inflammatory cells in the lamina propria of the ileum of Con, IR, IR + CM, IR + CA-CM, and IR + rEGF groups (0 = none, 1 = mild, 2 = moderate, 3 = high). (D) Body weights of Con, IR, IR + CM, IR + CA-CM, and IR + rEGF group were determined. (E) Immunohistochemistry against to epithelial barrier-related molecules, e.g., villin, zonula occuludens 1 (Zo1), desmoglein 2 (Dsg2), and claudin 3 (Cldn3), in the Con, IR, IR + CM, IR + CA-CM, and IR + rEGF group was performed. (F) mRNA levels of the epithelial barrier-related molecules in Con, IR, IR + CM, IR + CA-CM, and IR + rEGF group were assessed by qRT-PCR. Data are presented as the mean ± standard error of the mean; n = 5 mice per group. *P < 0.05 compared to the Con group; #P < 0.05 compared to the IR group. Scale bars represent 100 μm.

Supplementary Files

This is a list of supplementary files associated with this preprint. Click to download.

- CBsupplementFig1Jang.docx